



HAL
open science

High l double-Rydberg states $7d5/2nl$ of barium

P. Camus, J.-M. Lecomte, C. Mahon, P. Pillet, L. Pruvost

► **To cite this version:**

P. Camus, J.-M. Lecomte, C. Mahon, P. Pillet, L. Pruvost. High l double-Rydberg states $7d5/2nl$ of barium. *Journal de Physique II*, 1992, 2 (4), pp.715-725. 10.1051/jp2:1992161 . jpa-00247667

HAL Id: jpa-00247667

<https://hal.science/jpa-00247667>

Submitted on 4 Feb 2008

HAL is a multi-disciplinary open access archive for the deposit and dissemination of scientific research documents, whether they are published or not. The documents may come from teaching and research institutions in France or abroad, or from public or private research centers.

L'archive ouverte pluridisciplinaire **HAL**, est destinée au dépôt et à la diffusion de documents scientifiques de niveau recherche, publiés ou non, émanant des établissements d'enseignement et de recherche français ou étrangers, des laboratoires publics ou privés.

Classification
 Physics Abstracts
 31.50 — 32.80D

High ℓ double-Rydberg states $7d_{5/2}n\ell$ of barium

P. Camus, J.-M. Lecomte, C.R. Mahon, P. Pillet and L. Pruvost

Laboratoire Aimé Cotton *, C.N.R.S. II, Bâtiment 505, Campus d'Orsay, 91405 Orsay Cedex, France

(Received 30 October 1991, accepted 21 January 1992)

Resumé. — Une excitation du coeur isolé permet d'étudier les états double-Rydberg $7d_{5/2}n\ell$ du baryum pour n variant de 11 à 14 et ℓ de 7 à $n - 1$. L'état relais $6s n\ell$ est préalablement peuplé par une technique dite de débranchement adiabatique du champ électrique. Les spectres obtenus présentent une structure résolue dont l'origine est liée à l'existence d'une corrélation entre les deux électrons excités et que l'on identifie dans le couplage des moments angulaires $(j\ell)K$. Un calcul perturbatif incluant les termes d'interaction dipolaire et quadrupolaire permet d'obtenir les positions et les largeurs des raies. On observe un très bon accord entre théorie et expérience pour $\ell \geq 9$.

Abstract. — The $7d_{5/2}n\ell$ double-Rydberg states of barium have been studied for $n = 11$ to 14 and $\ell = 7$ to $n - 1$ using the Isolated Core Excitation technique along with a Stark switching method to populate the high ℓ states. The resulting spectra show resolved structures due to the correlation between the two excited electrons, identified by the $(j\ell)K$ angular momentum coupling between them. The spectra are compared to energy positions and linewidths calculated using a perturbative approach, including the dipole and quadrupole interaction terms. The agreement between experiment and theory is very good for high $\ell \geq 9$, but less so for lower ℓ .

1. Introduction.

The study of electron correlation effects in an atomic system with two excited electrons presents a particularly exciting problem in atomic physics. Double-Rydberg states ($N\ell_1n\ell$) allow one to study the evolution of correlation signatures when the two excited electrons have principal quantum numbers which begin to approach one another. Here we denote by N and n the principal quantum numbers, and ℓ_1 and ℓ the orbital angular momentum numbers of the inner and outer excited electrons, respectively.

In the extreme case for which $N \ll n$ the electrons are separated in space, and the system can be modelled as two independent electrons. Such states have been observed in barium

*This laboratory is associated with the Université Paris-Sud.

[1-5], strontium [6] and calcium [7] atoms and show little evidence for long range correlation between both excited electrons. They can be described using the quantum defect theory [8]. The theoretical interpretation of the spectra in this case is therefore quite straightforward.

The other extreme case is that of a strong correlation between the two electrons where $N \simeq n$. Several theoretical treatments such that the electrons are in a particular geometric configuration relative to the doubly charged core have been proposed [9, 10]. Experimentally correlated states first have been observed in the Helium atom [11] and more recently, with $N \simeq n$, in negative ions He^- [12, 13] and H^- [14] but have yet to be observed, to our knowledge, in neutral atomic systems.

The intermediate case where N and n begin to approach each other presents the onset of correlation and the breakdown of the independent particle model. Camus *et al.* [15] have recently demonstrated the onset of this correlation in barium atoms ($\ell_1, \ell \leq 2$) for $N \simeq 25$ and the ratio of the inner to outer electron effective principal quantum numbers $N^*/n^* \gtrsim 0.5$. This effect was shown to be due to the polarisation of the $\text{Ba}^+(N\ell_1)$ core in the presence of the multipole electric field created by the outer, $n\ell$, electron. In order to include the di-electronic interaction term into the Hamiltonian they used a method similar to a Born-Oppenheimer approximation. The polarisation of the core Ba^+ is treated with the outer electron frozen in position, and the outer electron wavefunction is then determined in a generalized MQDT approach taking into account the properties of the polarised core. Eichmann *et al.* [16] have also obtained similar results, showing a core polarisation effect of the outer electron on the $\text{Ba}^+(Nd$ or $Ng)$ core. Specifically, for $N \simeq 40$, $n \simeq 78$, excitation spectra for the inner electron were simulated on Ba^+ Rydberg states in the presence of a static electric field substituting the outer electron polarisation effect. However, high n and low ℓ were used, and the autoionisation linewidths were too large to enable the observation of the more subtle correlation manifestations between the two excited electrons [15-17].

In order to observe this kind of effects, Pruvost *et al.* [18] have recently studied the $6p_{3/2}n\ell$ and $6d_{5/2}n\ell$ ($n = 11 - 15$) states of Barium for which the outer electron has a high angular momentum, ($\ell = 6$ to $n - 1$). The autoionisation widths are small enough to demonstrate new correlation signatures. In these experiments $N^*/n \leq 0.33$ and the spectra show resolved structure identified as corresponding to the $(j\ell)K$ angular momentum coupling between the electrons. Here j denotes j_1 , the total angular momentum of the Ba^+ excited ion core and K the angular momentum defined by $\mathbf{K} = \mathbf{j}_1 + \ell$. The di-electronic interaction is treated theoretically as a perturbation to the independent electron Hamiltonian, taking into account the dipolar and quadrupolar terms in $1/r_{12}$ development, and within the $(j\ell)K$ coupling scheme. In general, it is interesting to examine the limits to this approach as the excitation of the inner electron is increased. We present here a study of the more highly excited $7d_{5/2}n\ell$ double-Rydberg states of barium for which $N^*/n \sim 0.4$. We first present in the next section our experimental technique and observations, followed in section 3 by a theoretical analysis and in section 4 a discussion of our results.

2. Experiment and observations.

The experimental set-up is similar to that used previously [4, 18], and so we include only a summary here. A beam of Barium atoms from an effusive source is laser excited between two electric field grids spaced 1 cm apart. To populate the $7d_{5/2}n\ell$ ($\ell = 7$ to $n - 1$) double-Rydberg states, we first use the Stark switching technique [6, 19] in order to selectively excite states of high ℓ and then the two-photon $6s_{1/2} \rightarrow 7d_{5/2}$ Isolated Core Excitation [20] (ICE) technique. The two-step excitation of the first, $6s^2$, Barium valence electron is achieved in the presence of an electric field of $F = 1000 - 1500$ V/cm. The first step is the $6s^2 \ ^1S_0 \rightarrow 6s6p$

1P_1 transition at 553.5 nm, and the second the $6s6p\ ^1P_1 \rightarrow 6s_{1/2}nk$ transition at $\simeq 429$ nm, where nk is a resolved Stark level of n . The electric field is then turned off sufficiently slowly so that as the Stark state $6snk$ adiabatically evolves into one of the non-degenerate zero field states, $6sn\ell$. The slow rate of the field is most critical near zero field where the Stark states are closest. We find that the condition of adiabaticity is met by an ‘‘exponential-like’’ turn-off of the field where it is first decreased by 90 % of its original value in $\simeq 1\ \mu\text{s}$, and the remaining 10 % in $\simeq 0.7\ \mu\text{s}$. At zero field the third laser is fired, exciting the $6s_{1/2}n\ell$ Rydberg atoms to the $7d_{5/2}n\ell$ double-Rydberg states. This two photon transition is close to the ionic $6s_{1/2} \rightarrow 7d_{5/2}$ two-photon line at 333.9 nm. We detect these states by monitoring the Ba^{2+} ion signal using a time of flight analyser. The predominant and detectable ionisation mechanism, in such an experiment, is photoionisation by an extra photon from the third laser of Ba^+ ions resulting from rapid ($\leq 10^{-9}$ s) autoionisation of the $7d_{5/2}n\ell$ states. The used UV light only photoionises Ba^+ ions in 5f and 8s states which are the most probable autoionisation channels. An electric field pulse is then applied to the bottom field grid in order to sweep all ions out of the interaction region through the upper grid and into a tandem microchannel plate detector. At the time of flight resolution of the detection system we easily discriminate between Ba^{2+} ions and the other laser produced ion signals.

Our method is to scan the frequency of the third laser in the neighbourhood of the ionic $6s_{1/2} \rightarrow 7d_{5/2}$ transition for a given $n\ell$ state of the outer electron. In figures 1 and 2, we show typical $7d_{5/2}n\ell$ spectra, in figure 1 for states of a given $\ell = 10$ with $n = 11 - 14$, and in figure 2 for $n = 11$ with ℓ varying from 7 to 10. Included in the spectra is the reference line $5s5p\ ^3P_1 \rightarrow 5s12s\ ^3S_1$ of Sr I [21]. The energy scale is given by use of a Fabry-Perot etalon. These spectra show a structure of several peaks which are interpreted as the result of the $(j_1\ell)K$ coupling between the $7d_{5/2}$ inner electron and the $n\ell$ outer one. In this coupling scheme, K varies from $\ell - j_1$ to $\ell + j_1$, which gives a possible maximum of 6 levels in our spectra. However, we note, in general, that the levels are not fully resolved except in cases $n = 11$ and $n = 12$, $\ell = 10$. This, to our knowledge, is the first time that the K components in the spectrum of such a highly excited double-Rydberg state have been resolved. Two features in figures 1 and 2 immediately stand out. The first is that the center of gravity of these states is systematically shifted to the red of the parent $6s_{1/2} \rightarrow 7d_{5/2}$ ionic line. This effect has been previously observed for $6pn\ell$ and $6dn\ell$ states, and is due to the small increase in the quantum defect of the $n\ell$ outer electron in the presence of a larger, excited, ion core, as compared to the smaller $6s_{1/2}n\ell$ state quantum defect. Second, we may follow the inverse ℓ dependence of the widths of the resonances. This dependence is simply a manifestation of the decreased penetration into the Ba^+ ion core with increased ℓ of the outer electron. For the higher ℓ , ≥ 9 , the autoionisation linewidths are probably below our two-photon excitation laser linewidth of $0.25\ \text{cm}^{-1}$, while for $\ell \leq 9$ the linewidths increase sharply, and for $\ell = 7$ we have only one single broad feature with a width of $\simeq 12\ \text{cm}^{-1}$.

The spectra of figures 1 and 2 show clearly the evolution of these double-Rydberg states as a function of the quantum numbers n and ℓ . For $n = 11$ and 12 , $\ell = 10$ all six components are completely resolved. In figure 1 we see that increasing n results in a decrease in the spacing between the K components. In figure 2 for $n = 11$, we note that for lower ℓ the energy separation between the K components increases indicating that the di-electronic coupling becomes stronger. This is clear if we consider that lower ℓ states, with a smaller centrifugal barrier, enable the outer electron to approach the inner, necessarily increasing the coupling.

We turn now in the next section to a theoretical interpretation of the energy positions and autoionisation widths of these resonances.

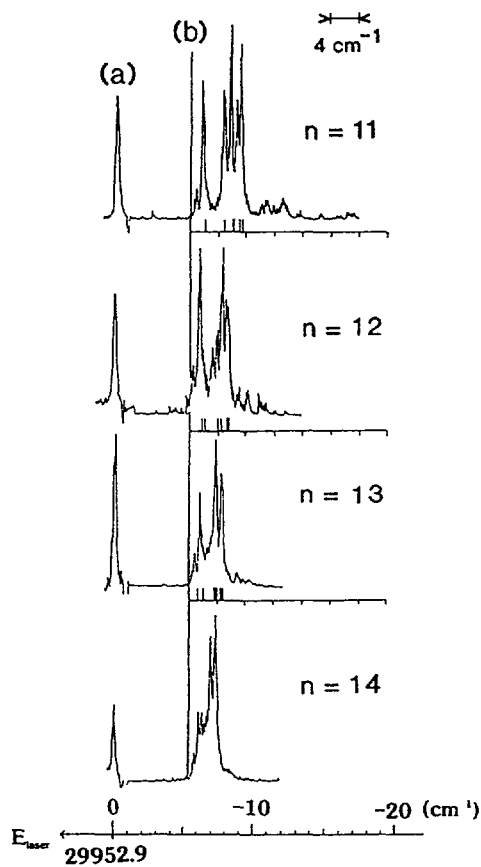


Fig. 1

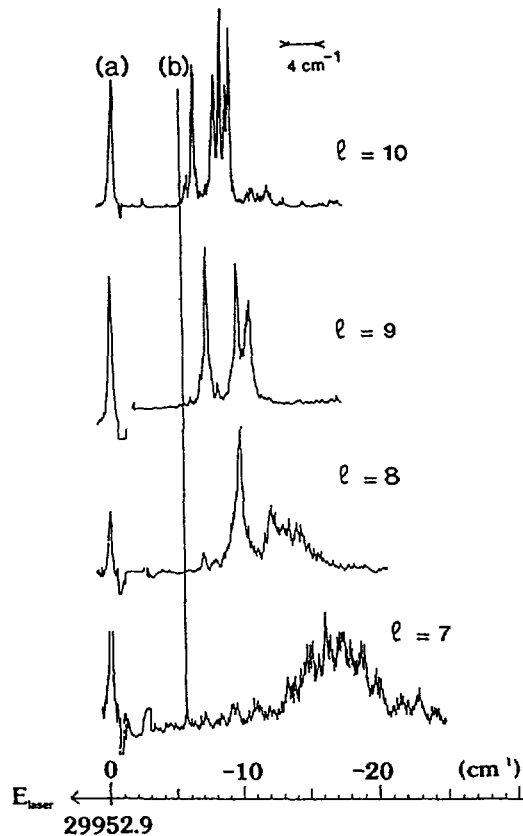


Fig. 2

Fig.1. — Two-photon excitation spectra $6s_{1/2}n\ell \rightarrow 7d_{5/2}n\ell$ for $\ell = 10$ and n varying from 11 to 14. (a) indicates the used reference line $5s5p\ ^3P_1$ ($E = 14504.351\text{ cm}^{-1}$) \rightarrow $5s12s\ ^3S_1$ ($E = 44457.3\text{ cm}^{-1}$) of Sr I [21]. (b) indicates the calculated position of the ionic line ($E = 59894.98\text{ cm}^{-1}$) [21], from the reference line (a). The line (b) does not appear on spectra because of the presence of an electric field before firing the excitation laser. Note that spectra energy scale is twice of laser one. The K energy positions are indicated by small straightlines with $K = 25/2, 15/2, 17/2, 23/2, 19/2, 21/2$ for $n = 12$ and 13 from left to right. For $n = 11$, the $25/2$ and $15/2$ are inverted and nearly blended (see Fig. 3a).

Fig.2. — Two-photon excitation spectra $6s_{1/2}n\ell \rightarrow 7d_{5/2}n\ell$ for $n = 11$ and ℓ varying from 7 to 10. (a) indicates the used reference line $5s5p\ ^3P_1$ ($E = 14504.351\text{ cm}^{-1}$) \rightarrow $5s12s\ ^3S_1$ ($E = 44457.3\text{ cm}^{-1}$) of Sr I. [21] (b) indicates the calculated position of the ionic line ($E = 59894.98\text{ cm}^{-1}$) [21], from the reference line (a). The line (b) does not appear on spectra because of the presence of an electric field before firing the excitation laser. Note that spectra energy scale is twice of laser one.

3. Theoretical treatment.

In the independent particle model the $7d_{5/2}n\ell$ states of Barium are completely degenerate. This system is comprised of a Ba^+ ion core with total angular momentum $j_1 = 5/2$ (i.e. the Ba^{2+} ion plus an "inner" $7d$ electron) about which orbits an "outer" Rydberg electron of orbital angular momentum ℓ . The inner electron moves in the field of the doubly charged Ba^{2+} core and has a large ($\simeq 2.4$) quantum defect. Its wavefunction only extends out from the core a few, $\simeq 25$ atomic units. The outer electron is essentially considered hydrogenic for large ℓ . Its wavefunction overlaps very little with that of the inner electron. As a result the interaction between both excited electrons is quite weak. Nevertheless, there is a small di-electronic interaction which lifts the degeneracy of these states, with the good quantum number being the total angular momentum of the system. The effect is typically on the order of 5 cm^{-1} , while the Δn energy spacing is on the order of 100 cm^{-1} . For this reason the system may be treated using perturbation theory in the $(j\ell)K$ scheme defined in the previous section. We neglect here the spin of the outer electron. Due to the small overlap of the wavefunctions of the two electrons we may also neglect the exchange effects.

We use the two-electron Hamiltonian

$$H = \left[-\frac{\Delta_1}{2} + V(r_1) + \zeta_1 \mathbf{l}_1 \cdot \mathbf{s}_1\right] + \left[-\frac{\Delta_2}{2} + V(r_2)\right] + \frac{1}{r_{12}} \quad (1)$$

Only the spin-orbit interaction for the first ("inner") electron is taken into account. The closed-shell core Ba^{2+} -electron interaction is described by a simple model potential $V(r)$ [22]. The di-electronic interaction is developed into the multipolar expansion using the q rank tensorial operators $C^q(\theta, \phi)$

$$\frac{1}{r_{12}} = \sum_{q=0}^{\infty} \frac{r_{<}^q}{r_{>}^{q+1}} C^q(\theta_1, \phi_1) \cdot C^q(\theta_2, \phi_2) \quad (2)$$

where $r_{>} = \max(r_1, r_2)$, and $r_{<} = \min(r_1, r_2)$. The total Hamiltonian commutes with K^2 and K_z as well as the parity operator.

In a first step we determine, for a given K , simultaneously the radial motion of the inner electron, as well as the total angular motion of the system. For this system we define the functions $\Phi_i(r_1, \Omega)$ ($\Omega = (\hat{r}_1, \hat{r}_2)$) as the collisional channels $i = \{(N_1 \ell_1)_{j_1} \ell K\}$. The radial part of this function is solution of a one electron Schrödinger equation which depends on the potential $V(r)$. This potential includes a screening term and a polarisation term, both terms being ℓ dependent:

$$V_\ell(r) = -\frac{1}{r} [I + (Z - I) \exp(-\alpha_1^\ell r) + \alpha_2^\ell r \exp(-\alpha_3^\ell r)] - \frac{\alpha_d}{r^4} [1 - \exp(-(\frac{r}{r_c^\ell})^6)] \quad (3)$$

I is the ion charge (here $I = 2$), Z is the atomic number of barium and α_d is the polarisability of the Ba^{2+} ion. The empirical parameters α_i^ℓ and r_c^ℓ are adjusted until the energy levels of the Schrödinger equation reproduces accurately the average spin-orbit energies of the Ba^+ s, p, d, f experimental levels [23]. For $\ell \geq 4$, we use the f-potential.

We construct the zero order wavefunctions as the product of the core-wavefunction Φ_i by a radial wavefunction $F_i^n(r_2)$. This function is solution of the Schrödinger equation taking into account the monopolar and diagonal quadrupolar potential caused by the inner electron in the state Φ_i

$$\left[-\frac{1}{2} \frac{d^2}{dr^2} + \frac{\ell(\ell+1)}{2r^2} + V_\ell(r) + y_0(i, i, r) + \alpha_{ii}^{Kq=2} y_2(i, i, r)\right] F_i^n(r) = \varepsilon_i F_i^n(r) \quad (4)$$

$\varepsilon_i = -1/2n^{*2}$ where n^* is a effective quantum number. $y_q(i, i', r)$ are the Hartree functions

$$y_q(i, i', r_2) = \int_0^\infty p_i(r_1) p_{i'}(r_1) \frac{r_1^q}{r_2^{q+1}} r_1^2 dr_1, \quad (5)$$

where $p_{i'}$ and p_i are the radial parts of the wavefunctions $\Phi_{i'}$ and Φ_i respectively. $\alpha_{ii'}^{Kq}$ is an angular coefficient

$$\alpha_{ii'}^{Kq} = \langle (N\ell_1)_{j_1} \ell K \parallel C_1^q \cdot C_2^q \parallel (N'\ell'_1)_{j'_1} \ell' K' \rangle \delta_{KK'} \quad (6)$$

For very large r_2 , i.e. $r_2 \gg r_1$, or for $r_2 > 2N^{*2}/I^2$ (N^* is the effective principal quantum number of the inner electron), the asymptotic form of y_q is

$$y_q(i, i', r_2) \sim \frac{1}{r_2^{q+1}} \int_0^\infty p_i(r_1) p_{i'}(r_1) r_1^{q+2} dr_1. \quad (7)$$

The zero order wavefunctions are not degenerate. The choice of these zero order wavefunctions enables us to take into account one part of the channel coupling. In the case of the $6pn\ell$ [18] this part (i.e. the intrachannel quadrupolar coupling) is the most important perturbation potential and the experimentally observed states correspond to the zero order wavefunctions.

The wavefunctions corresponding to two different i and i' channels are coupled each other by the multipolar (essentially dipolar) potential term $\sum_q \alpha_{ii'}^{Kq} y_q(i, i', r)$ where the summation extends over all values of q except $q = 0$ and, if $i = i'$, $q = 2$. The effects of this coupling are calculated only in the frame of the second order perturbation theory. The zero order wavefunctions being not degenerate, we use the non-degenerate perturbative theory.

4. Comparison of second order perturbative calculations and experiments and discussion.

We account for dipole and quadrupole terms in our calculations and include $\simeq 80$ channels between the limits $6s$ and $7f$ of Ba^+ . In figure 1 the calculated energy positions of the K components of the $7d_{5/2}n\ell$ states are compared to the experimental structures for ℓ fixed and different values of n . In figure 3 we show the spectra simulated from our perturbation theory calculations, and assuming that the starting level for laser excitation, $6sn\ell \ ^1L$, is pure (the mixing with the 3L states is unknown). For autoionisation widths of less than 0.5 cm^{-1} we use the experimental laser linewidth. The agreement between the simulated and experimental spectra is very good for $\ell \geq 10$. The spacing between the K components is reproduced by the theory. We have observed a systematic shift $\sim 0.4 \text{ cm}^{-1}$ identical for all the spectra compatible with the experimental errors. We have noticed that the major perturbators to the $7dn\ell$ states are the channels corresponding to the core in a state $8p$, $6f$, or $5f$.

At the same time, the autoionisation widths are calculated using the Fermi golden rule. The $5f$ and $8s$ channels contribute the most to the autoionisation widths of these states. These widths decrease very rapidly with ℓ for fixed n and K (Fig. 5a). The decreasing rate calculated is in agreement with the calculations done on $6pn\ell$ or $5dn\ell$ of barium using hydrogenic outer wavefunctions [24]. On the other hand for fixed ℓ and K the widths increase with n (Fig. 5b). This is due to the fact that for increased n the inner turning point decreases and the interaction for small r with the continuum functions increased rapidly.

It is worthwhile at this point to discuss several of the assumptions and approximations made in carrying out these calculations. We have also examined the contributions from higher order multipolar terms and remark that for the $\ell \geq 10$ states studied here the octupolar terms are

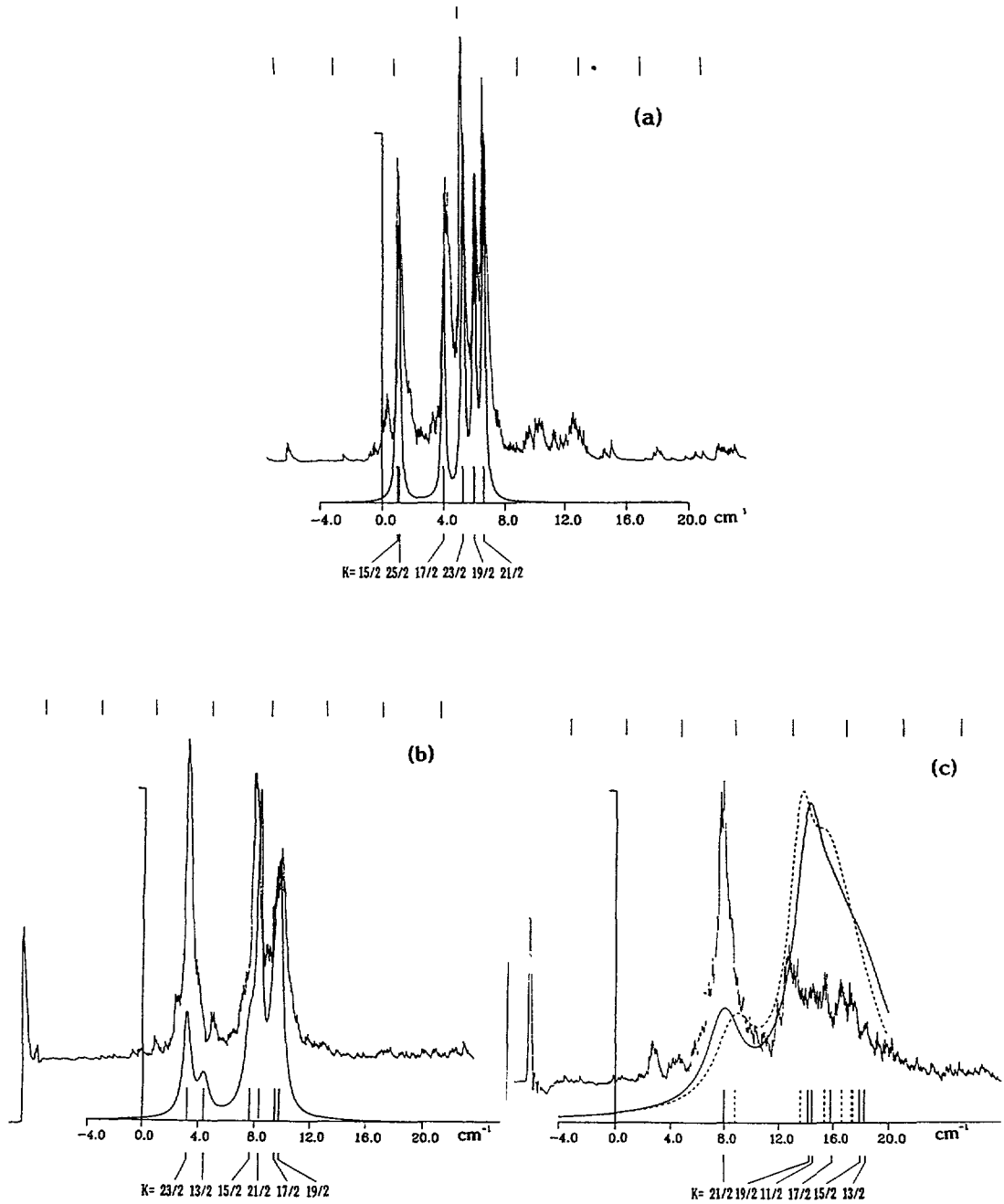


Fig.3. — Comparison of experimental and theoretical spectra $6s_{1/2}n\ell \rightarrow 7d_{5/2}n\ell$ for $n = 11$ and $\ell = 10$ (a), 9 (b) and 8 (c). The small straightlines indicate the K energy positions. The dashed curve of figure (c) has been obtained using a calculation with no perturbation within the perturbing channels.

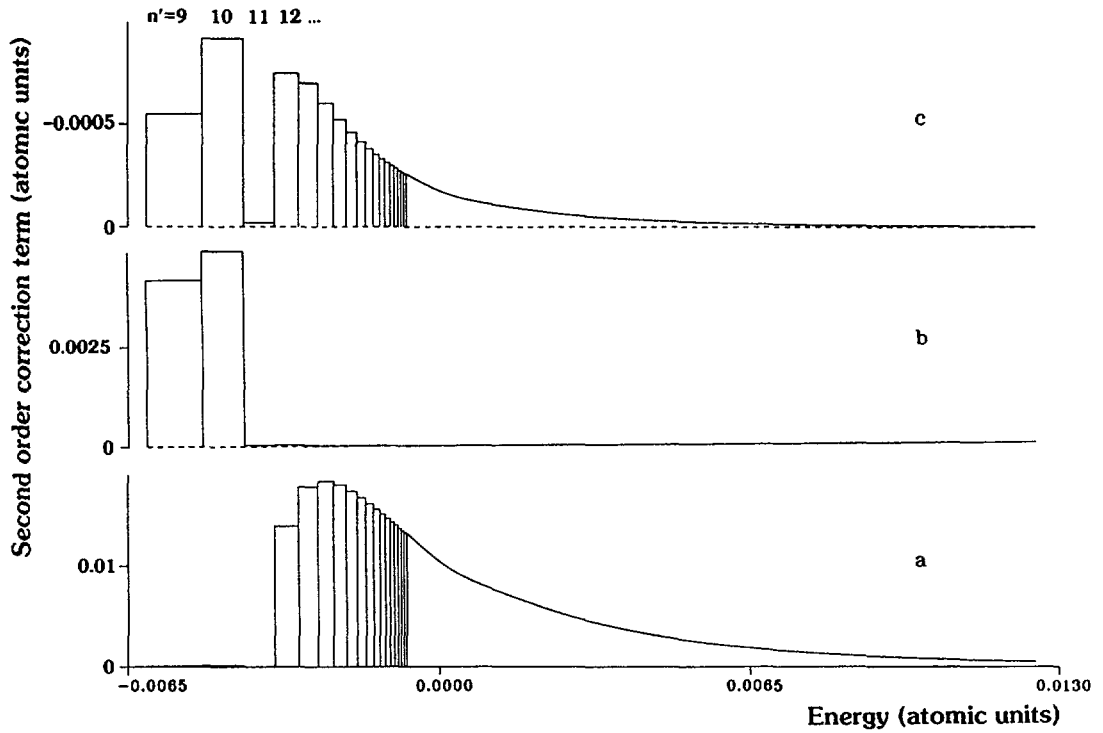


Fig.4. — Comparison of diagonal and non-diagonal second order contributions for $8p_{3/2}n'\ell'$, $K=19/2$ perturbing $7d_{5/2}$, $n=11$, ℓ , $K=19/2$ as a function of the energy $-1/2n'^{-2}$: (a) direct term, $7d_{5/2}$, $n=11$, $\ell=7$, $K=19/2$ coupled to $8p_{3/2}n'$, $\ell'=8$, $K=19/2$. (b) direct term, $7d_{5/2}$, $n=11$, $\ell=9$, $K=19/2$ coupled to $8p_{3/2}n'$, $\ell'=8$, $K=19/2$. (c) cross term, $7d_{5/2}$, $n=11$, $\ell=7$, $K=19/2$ which is coupled to $8p_{3/2}n'$, $\ell'=8$, $K=19/2$ which is coupled to $7d_{5/2}$, $n=11$, $\ell=9$, $K=19/2$. Note that the vertical scales are different for the three figures.

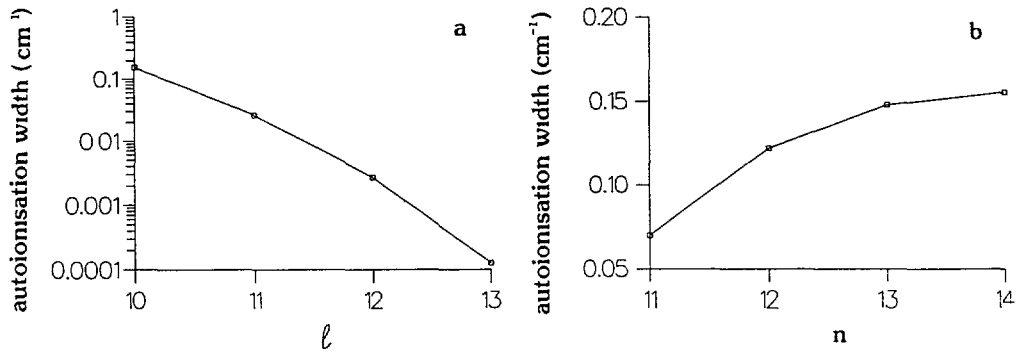


Fig.5. — Calculated autoionisation widths (in cm^{-1}) (a) vs. ℓ for $n = 14$ and $K = \ell + 5/2$. Note the vertical logarithmic scale. (b) vs. n for $\ell = 10$ and $K = \ell + 5/2$.

typically at least two orders of magnitude lower than the quadrupolar terms, and therefore higher multipole moments may be neglected to good approximation. The calculations take into account the penetration of the outer orbit into the Ba^+ core. However we have noticed that there is no significant difference in the results when the y_q functions are reduced to their asymptotic parts. This therefore justifies our neglect of the exchange terms.

Hereafter, the use of the non-degenerate perturbative theory is questioned. The different states $|7d_{5/2}, n\ell K\rangle$ of the same n and K belong to the same non-degenerate multiplet. We note that the first order terms of the perturbation theory introduce corrections of the same order of magnitude as the separation between the zero order states. In principle it should, therefore, be necessary to treat the problem by considering the zero order states as quasi-degenerate, and not non-degenerate as we have done.

To first order the elements of the same multiplet are, in principle, coupled by the non-diagonal quadrupolar terms. Their coupling is in general smaller than their spacing, and is strictly zero if $y_q(i, i', r_2)$ is reduced to its asymptotic form and the outer electron wavefunctions are purely hydrogenic because of the well-known orthogonalisation relation between radial hydrogenic functions [25]. We neglect the non-hydrogenic coupling, which introduces a very small ($\leq 0.1\%$) mixing. In the helium atom the fundamental role of this relation is pointed out in [26]: then, the angular momentum of the external electron ℓ is approximately a "good quantum number". However the case of barium atom is quite different from the case of He. In the latter system the degeneracy between levels corresponding to different degenerate states of the first, internal, electron induces a large mixing between different configuration states. In our case, due to the non-hydrogenic character of inner electron wavefunction for barium the $|7d_{5/2} n\ell K\rangle$ states are generally non-degenerate with the $|(N\ell_1)_{j_1} n\ell K\rangle$ where $(N\ell_1)_{j_1} \neq 7d_{5/2}$. However we have noticed that for lower ℓ accidental quasi-degeneracy can happen. For example, the coupling between the levels $|7d_{5/2}, n = 11, \ell = 7, K = 17/2\rangle$ and $|8p_{3/2}, n = 7, \ell = 6, K = 17/2\rangle$ is on the same magnitude order as their spacing. In such cases (which appear systematically for $\ell \leq 7$) our non-degenerate perturbation theory is no longer available.

Moreover, the second order introduces mixing terms between $7d_{5/2} n\ell$ and $n\ell \pm 2$ states for the same K . For evaluating the order of magnitude of the ℓ -coupling term we study the behaviour of the matrix elements of an irregular potential (like $1/r^2$) between one-electron purely hydrogenic functions such as $\langle n\ell | 1/r^2 | n'\ell - 1 \rangle$ and $\langle n\ell - 2 | 1/r^2 | n'\ell - 1 \rangle$. For n and ℓ fixed their distributions as a function of n' are very asymmetric: the first matrix element is large for $n' < n$ and negligible for $n' > n$, on the contrary the second one is important only when $n' > n$. This important property is kept though the outer wavefunctions are non-hydrogenic. Then we study the contributions up to the second order of the same perturbing channel states on two perturbed states $7d_{5/2}n\ell$ and $\ell - 2$. As it is explicit in figure 4 and also in figures 10 and 11 of the reference [27] there is a large dissymmetry in the distribution of these perturbing states, implying that the crossterm, which is responsible to the ℓ -mixing, is therefore much smaller than the direct terms, introducing only an at most 1 % mixing effect. Let us remark, at this point, that for the same reasons the continuum states which contribute the most to the linewidths are those with angular momentum $\ell+1$ or $\ell+2$, as it is pointed out in [24], i.e. $|(5f)_{5/2, 7/2} n'(\ell+1) K\rangle$ or $|(8s_{1/2} n'(\ell+2) K\rangle$.

Consequently, in the case of smaller ℓ and K values, the states $|7d_{5/2} n\ell K\rangle$ are coupled to states of low angular momentum $\ell-1$ or $\ell-2$ for which the hydrogenic character of the outer electron wavefunction is smaller and the coupling may be non negligible. For example, for $K = 11/2$ ($n, \ell = 8$) coupled with ($n, \ell = 6$) which is in turn coupled to ($n, \ell = 4$), and a more complete theoretical treatment is required to describe the system. In addition the states involved are more penetrating into the Ba^+ core and the effects of other multipolar coupling than the di- and quadrupolar must be calculated.

A last approximation involves our use of the zero order perturbed wavefunctions. Starting with zero order hydrogenic functions for the outer electron we have done another second order perturbative calculation. In the first calculation the quadrupolar interaction within the perturbed ($7d_{5/2}$) and all the perturbing channels are accounted for. In the second calculation there is no perturbation within the perturbing channels. We note no difference in the two calculations for large values of ℓ but the effect on the line-positions and on the autoionisation widths becomes more pronounced as ℓ is decreased as shown in figure 3c. The perturbation theory appears, therefore, to have reached a limit of applicability since it does not take into account the interaction between the perturbing channels, coupled dipolar in general, but which have an effect may be as large as or greater than the quadrupolar intra-channel coupling.

5. Conclusion.

In conclusion, we have presented an analysis of the $7d_{5/2}n\ell$ spectra using an extension of the perturbation method applied for the $6pn\ell$ and $6dn\ell$ states. Our results show that for $\ell \geq 9$ the theory reproduces the spectra very well. Decreasing ℓ , or increasing n (at ℓ fixed the outer electron is more delocalised) or increasing N , the excitation of the inner electron, then the radial separation of the inner and outer orbits becomes less pronounced and the coupling within all the channels and between them are increasing. It is therefore necessary to take into account all the channel coupling effects, and this requires a method overpassing the perturbation theory. We believe, in particular, that the autoionisation widths are very sensitive to these effects and only such calculations should be performed in order to explain the discrepancies between experiment and calculation for low ℓ .

We have noticed that the lack of ℓ -mixing in the same multiplet is due to the quasi-hydrogenic character of the radial function of the outer electron. If the excitation of the inner electron is increased, the hydrogenic character disappears and the orthogonalisation relation between radial functions [25] may be damaged and a larger ℓ -mixing is then produced. An adaptation of the R -matrix theory to the large angular momenta is in progress, which will allow us to check this point for more excited states e.g. $8dn\ell$.

Acknowledgements.

It is a pleasure to thank G. Hubbard for the excellent technical assistance and M. Aymar for providing the parametric potential of Ba^+

References

- [1] Tran N.H., Pillet P., Kachru R. and Gallagher T.F., *Phys. Rev. A* **29** (1984) 2640.
- [2] Pruvost L., Bolovinos A., Camus P., Lecomte J.-M. and Pillet P., *J. Phys. B: At. Mol. Opt. Phys.*, **23** (1990) L95.
- [3] Bente E.A.J. and Hogervorst W., *J. Phys. B: At. Mol. Opt. Phys.*, **22** (1989) 2679.
- [4] Camus P., Pillet P. and Boulmer J., *J. Phys. B: At. Mol. Opt. Phys.* **18** (1984) L481.
- [5] Jopson R.M., Freeman R.R., Cooke W.E. and Bokor J., *Phys. Rev. Lett.* **51** (1983) 1640.
- [6] Cooke W.E., Gallagher T.F., Edelstein S.A. and Hill R.M., *Phys. Rev. Lett.* **40** (1978) 178.
- [7] Morita N. and Suzuki T., *J. Phys. B: At. Mol. Opt. Phys.* **21** (1988) L439.
- [8] Seaton M.J., *Rep. Prog. Phys.* **46** (1983) 167.
- [9] Herrick D.R., *Phys. Rev. A* **24** (1981) 161.
- [10] Watanabe S. and Lin C.D., *Phys. Rev. A* **34** (1986) 823.

- [11] Madden R.P. and Codling K., *Phys. Rev. Lett.* **10** (1963) 518.
- [12] Buckman S.J., Hammond P., Read F.H. and King G.C., *J. Phys. B: At. Mol. Opt. Phys.* **16** (1983) 4039.
- [13] Buckman S.J. and Newman D.S., *J. Phys. B: At. Mol. Opt. Phys.* **20** (1987) L711.
- [14] Harris P.G., Bryant H.C. and Mohagheghi A.H. *et al.*, *Phys. Rev. Lett.* **65** (1990) 309.
- [15] Camus P., Gallagher T.F., Lecomte J.-M., Pillet P., Pruvost L. and Boulmer J., *Phys. Rev. Lett.* **62** (1989) 2365.
- [16] Eichmann U., Lange V. and Sandner W., *Phys. Rev. Lett.* **3** (1990) 274.
- [17] Jones R.R. and Gallagher T.F., *Phys. Rev. A* **42** (1990) 2655.
- [18] Pruvost L., Camus P., Lecomte J.-M., Mahon C.R. and Pillet P., *J. Phys. B: At. Mol. Opt. Phys.* **22** (1991) 4723.
- [19] Freeman R.R. and Kleppner D., *Phys. Rev. A* **20** (1976) 2251.
- [20] Cooke W.E. and Gallagher T.F., *Phys. Rev. Lett.* **41** (1978) 1648.
- [21] Moore C.E., Atomic Energy Levels, III, NSR DS-NBS 35 (1971).
- [22] Klapisch M., *Comput. Phys. Common* **2** (1971) 239.
- [23] Aymar M., *J. Phys. B: At. Mol. Opt. Phys.* **23** (1990) 2697.
- [24] Poirier M., *Phys. Rev. A* **38** (1988) 3484.
- [25] Pasternack S. and Sternheimer R.M., *J. Math. Phys.* **3** (1962) 1280.
- [26] Nikitin S.I. and Ostrovski V.N., *J. Phys. B: At. Mol. Opt. Phys.* **9** (1976) 3141.
- [27] Gallagher T.F., Kachru R. and Tran N.H., *Phys. Rev. A* **26** (1982) 2611.